APPLIED AND ENVIRONMENTAL MICROBIOLOGY, Mar. 2004, p. 1434–1441 Vol. 70, No. 3
0099-2240/04/$08.00+0 DOI: 10.1128/AEM.70.3.1434–1441.2004

Symbiont-Induced Changes in Host Actin during the Onset of a Beneficial Animal-Bacterial Association

Jennifer R. Kimbell and Margaret J. McFall-Ngai*

Pacific Biomedical Research Center, Kewalo Marine Laboratory, University of Hawaii, Honolulu, Hawaii

Received 9 October 2003/Accepted 1 December 2003

The influence of bacteria on the cytoskeleton of animal cells has been studied extensively only in pathogenic associations. We characterized changes in host cytoskeletal actin induced by the bacterial partner during the onset of a cooperative animal-bacteria association using the squid-vibrio model. Two-dimensional sodium dodecyl sulfate-polyacrylamide gel electrophoresis and Western blot analysis revealed that *Vibrio fischeri* induced a dramatic increase in actin protein abundance in the bacteria-associated host tissues during the onset of the symbiosis. Immunocytochemistry revealed that this change in actin abundance correlated with a two- to threefold increase in actin in the apical cell surface of the epithelium-lined ducts, the route of entry of symbionts into host tissues. Real-time reverse transcriptase PCR and in situ hybridization did not detect corresponding changes in actin mRNA. Temporally correlated with the bacteria-induced changes in actin levels was a two- to threefold decrease in duct circumference, a 20% loss in the average number of cells interfacing with the duct lumina, and dramatic changes in duct cell shape. When considered with previous studies of the biomechanical and biochemical characteristics of the duct, these findings suggest that the bacterial symbionts, upon colonizing the host organ, induce modifications that physically and chemically limit the opportunity for subsequent colonizers to pass through the ducts. Continued study of the squid-vibrio system will allow further comparisons of the mechanisms by which pathogenic and cooperative bacteria influence cytoskeleton dynamics in host cells.

Studies of beneficial and pathogenic bacteria have demonstrated that bacteria can dramatically influence the morphology, biochemistry, and molecular biology of host tissues with which they associate (13). Principal targets of such modifications are the polarized epithelial cells that line mucosal surfaces, the sites of first and often persistent interaction with bacterial cells (18). Among the changes in host epithelial cells that result from interaction with bacterial pathogens, perhaps the most conspicuous and well studied are the modifications of the host cell cytoskeleton (1, 8). By altering the host cytoskeleton, often through the activity of a secreted toxin or a factor injected into the host cell, various pathogens increase their intimacy with the host tissues, i.e., gain entry into cells, increase membrane contact with the cell surface, or invade tissues by disrupting junctions between cells. For example, enterohemorrhagic *Escherichia coli* rearranges the cytoskeleton of the host intestinal epithelium, which results in the formation of apical surface pedestals where the pathogen resides extracellularly (9).

Most studies of the interactions of bacteria with polarized epithelia have been restricted to the influence of pathogens on cultured mammalian cells (18). However, as the community of biologists increasingly recognizes the importance of beneficial bacteria in the health and disease of humans and other animals (15, 33, 34), models are being developed to characterize the nature of the interplay between the epithelial cells and their coevolved bacterial partners (10, 14, 20). One such model is the exclusive partnership between the host squid *Euprymna scolopes* and the luminous bacterium *Vibrio fischeri*. This system offers a relatively simple experimental model for the study of persistent colonization of epithelia by extracellular bacteria in an intact association (23, 40). Both partners can be cultured independently under laboratory conditions, and molecular genetic methods have been developed for the bacterial symbiont.

Similar to the acquisition by mammals of their microbiota following birth, each generation of host squid acquires *V. fischeri* from the environment within hours of hatching from the egg (31). During embryogenesis, superficial ciliated fields that potentiate the colonization process develop on either side of the incipient light organ (Fig. 1A) (26, 31). At hatching, the cells of these fields secrete mucus within which *V. fischeri* aggregates for the first 2 to 3 h (32). The harvested *V. fischeri* are suspended by the cilia of the epithelial cells above a series of pores at the base of the appendages (Fig. 1B). At 3 to 4 h posthatching, amassed *V. fischeri* cells follow a path through these pores, travel down ciliated ducts, and colonize deep epithelium-lined crypts on each side of the light organ (Fig. 1C and D).

Beginning with passage through the ducts and the onset of colonization of the crypt spaces, *V. fischeri* induces a sequence of widespread developmental changes in the host light organ over the first hours to days (40). Using antibiotics to cure the light organ of *V. fischeri*, these modifications of host tissue have been found to be either reversible, i.e., constant exposure to *V. fischeri* is required to maintain these changes, or irreversible, i.e., a transient interaction with the symbiont is sufficient to induce morphological changes. Specifically, the crypt epithelium, which interfaces directly with the symbionts, undergoes a reversible increase in the microvillar density of the apical sur-

* Corresponding author. Mailing address: Pacific Biomedical Research Center, Kewalo Marine Laboratory, 41 Ahui St., Honolulu, HI 96813. Phone: (808) 539-7310. Fax: (808) 599-4817. E-mail: mcfallng@hawaii.edu.

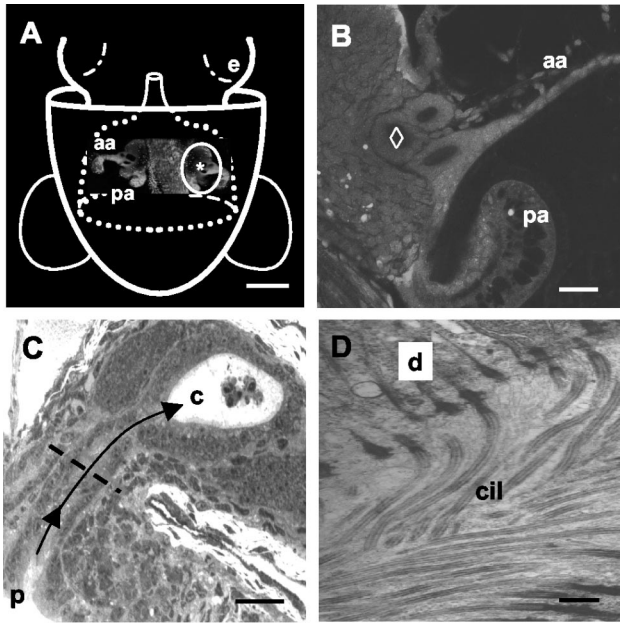

FIG. 1. *V. fischeri* must travel down narrow, ciliated ducts to colonize the light organ of *E. scolopes*. (A) Schematic of a ventral view of a hatchling squid superimposed over a confocal micrograph of the light organ (e = eye). The light organ is circumscribed by the posterior portion of the funnel (dotted white lines) (modified from reference 31). The pores (*) leading to the ducts of the organ are located at the base of a pair of "appendages" (aa = anterior appendage; pa = posterior appendage), components of two complex ciliated fields, one on each lateral surface of the organ (circled in white), that facilitate colonization by symbionts. Bar, 250 μm. (B) Higher-magnification confocal image of one side of the organ in the region of the ducts. The most medial duct (◊) was used for all analyses in the present study. Bar, 25 μm. (C) Histological section of an uninfected juvenile light organ. Each pore (p) is an opening to a ciliated, microvillous duct that leads (arrows) to one of three epithelium-lined crypts (c) on each side of the light organ. In the crypts, the bacteria interact with the epithelium and a population of macrophage-like hemocytes, which appear in this image as central in a crypt space. The dashed line indicates the position in the duct at which all confocal analyses were performed. Bar, 25 μm. (D) Transmission electron micrograph demonstrating the density of cilia (cil) along the duct (d = duct epithelial cell). Bar, 2 μm.

faces of the crypt cells (21) and an induction of edema in these cells (41). In contrast, the superficial ciliated fields, which are remote from the symbionts occupying the crypt spaces, undergo a 4-day program of regression that only requires a 12-h exposure to the symbionts (4, 27). In addition to these initial events, the symbiosis is characterized by a daily rhythm (12, 29). The pores and ducts remain open throughout the life of the host, and each day ~90% of the bacterial population is vented from the light organ crypts through the ducts into the surrounding environment; the population that remains behind in the organ is the principal inoculum that will grow and fill the crypts by the end of the day. In the absence of *V. fischeri*, the organs of aposymbiotic animals (i.e., uncolonized animals that have been exposed to seawater with nonsymbiotic marine bacteria) do not become colonized (24).

Molecular phylogenetic and experimental studies of squid-vibrio symbioses have demonstrated that these associations are highly specific (19, 28). Characterizations of the *E. scolopes-V. fischeri* system indicate that the duct plays a central role in this specificity. Whereas other gram-negative bacteria will associate with the mucus secreted by the light organ during aggregation, they are inhibited from entering host tissues at the pores (31). Studies of the morphology and biochemistry of the ducts have provided evidence that they present a biomechanical and biochemical gauntlet. The apical surfaces of the duct cells are densely covered with cilia and microvilli, and the cilia beat outward (25). *V. fischeri* mutants defective in motility (11) will aggregate at the pores but do not progress into the ducts (30, 31). In addition, the epithelial cells lining the ducts present high levels of oxidative stress conferred by an abundance of halide peroxidase and nitric oxide synthase (36; S. K. Davidson, R. Kossmehl, and M. J. McFall-Ngai, Abstr. 101st Gen. Meet. Am. Soc. Microbiol., abstr. N-107, 2001).

This study reports symbiont-induced changes in the actin cytoskeleton of the duct cells and provides evidence that these changes may work in concert with the other duct defenses to restrict entry into host tissues. Specifically, we (i) characterized actin gene expression at the level of transcription and translation in the *E. scolopes* light organ ducts during the onset of the association with *V. fischeri*; (ii) localized changes by immunocytochemistry and in situ hybridization; (iii) determined whether such changes are reversible or irreversible; and (iv) correlated these changes with symbiont-induced changes in duct dimensions and duct cell architecture. The results of these studies support the use of the *E. scolopes-V. fischeri* model for the study of bacteria-altered host cytoskeleton in an intact, beneficial association.

MATERIALS AND METHODS

General procedures. Juvenile squid were obtained from egg clutches that were maintained in open-flow seawater tables as previously described (4). Newly hatched squid were made symbiotic by incubating them in offshore seawater to which ~10^3 *V. fischeri* ES114 cells/ml were added for 12 h, followed by maintenance in Hawaiian seawater that did not contain sufficient quantities of *V. fischeri* to result in colonization. Squid were maintained in this offshore seawater immediately upon hatching to maintain them as aposymbiotic. All animals were kept individually in glass scintillation vials, and the seawater was changed daily. To confirm the presence or absence of symbiosis in host animals, the luminescence of the animals, which results from induction of luminescence in colonizing *V. fischeri*, was assessed daily by measuring light output with a photometer (model 20/20; Turner Designs, Sunnyvale, Calif.). In experiments where light organs were cured of their symbionts, the antibiotic chloramphenicol (CM) was used at 20 μg/ml of seawater (4). A CM-resistant strain of *V. fischeri*, ES114(pVO8), was used as a control for any pharmacological effects that CM treatment may have on the light organ tissues (39). Chemicals and antibodies were purchased from Sigma-Aldrich Chemical Co. (St. Louis, Mo.) unless otherwise stated.

Confocal microscopy. All confocal experiments were performed on a Zeiss LSM 510 system. In comparisons of fluorescence intensity, a ratio of duct fluorescence intensity over the fluorescence intensity of background tissue was calculated for each specimen. Dimensions of tissue features, as well as the intensity of cross-reactivity of fluorochromes, were determined using Zeiss LSM 510 software version 2.8. All measurements were conducted on the medial duct (Fig. 1B). The ducts develop sequentially over embryogenesis (26). At hatching, the medial duct is the most fully developed and leads to the most fully developed crypt. The less mature ducts and crypts have more anatomical variation than the medial duct and crypt. For each determination of fluorescence intensity within a duct cross-section, a 20-μm length of the brightest area was measured. All measurements were conducted below the level of saturation of the detector.

2-D PAGE. To prepare extracts of squid tissue for two-dimensional polyacrylamide gel electrophoresis (2-D PAGE) of unlabeled proteins, the juvenile squid were anesthetized in 2% ethanol in seawater. The light organs were dissected from the mantle cavity of the animal and accumulated in 50 mM Tris buffer (pH 7.2) on ice and then homogenized with a glass micromortar and pestle. The homogenate was centrifuged at 14,000 × *g* for 15 min at 4°C to remove bacterial cells, animal membranes, and squid ink. The soluble fraction was removed, and

the protein concentration was determined spectrophotometrically. Twenty micrograms of soluble protein sample was prepared for isoelectric focusing by adding four parts of lysis solution (8 M urea, 1% dithiothreitol, 2% Pharmalyte 3-10, 0.05% Triton X-100, 0.14% phenylmethylsulfonyl fluoride; pH 7.4) to one part protein sample. We used the Pharmacia LKB Multiphor II 2-D electrophoresis system with precast Immobilon dry strip isoelectric focusing gels (linear pH gradient of 4 to 7 or 4.5 to 5.5) and ExcelGel (12 to 14% gradient) sodium dodecyl sulfate (SDS)-polyacrylamide gels. The gels were run and stained as previously described (5).

For 2-D PAGE of ^{35}S-radiolabeled proteins, prior to labeling squid were preincubated in 10 μg of CM/ml for 30 min to inhibit protein synthesis of the bacterial symbionts. Squid were then incubated for 2 h with ICN Tran^{35}S-label, which contains 70% L-[^{35}S]methionine. Thirteen microcuries of label was used per squid. Squid were first rinsed twice for several seconds and then once for 1 h in seawater supplemented with 8 mM methionine. 2-D PAGE gels of the soluble proteins were run as described above, and proteins that had incorporated radiolabel were visualized by autoradiography. Experiments were done in triplicate to confirm reproducibility of the results.

Western blot analyses. For protein-antibody hybridizations, relevant sections of the 2-D PAGE gels were electrophoretically transferred to nitrocellulose membranes (0.45-μm pore size) at 15°C for 1 h at 200 mA in transfer buffer (25 mM Tris-HCl, 200 mM glycine, 20% methanol; pH 8.3). The membranes were then blocked overnight in Tris-buffered saline (TBS; 20 mM Tris with 0.5 M NaCl; pH 7.4) with 3% bovine serum albumin (BSA), followed by incubation with a 1:50 dilution of a polyclonal antibody (catalog no. A2066; Sigma-Aldrich Chemical Co.) to the conserved C-terminal 11 amino acids of the actin molecule in 1% BSA–Tween-TBS (TTBS) overnight. They were then rinsed three times for 10 min in TBS and incubated for 45 min in goat anti-rabbit antibody conjugated to horseradish peroxidase (1:3,000) in 1% BSA–TTBS at room temperature and then rinsed three times for 10 min in TTBS at room temperature. Cross-reactivity with the antiactin antibody was visualized by chemiluminescence (Renaissance Western blot chemiluminescent kit; NEN Life Science Products, Boston, Mass.). One hundred nanograms of control actin from chicken was loaded onto the second dimensions of the 2-D gels as a positive control.

Immunocytochemistry. Squid were anesthetized in 2% ethanol in seawater and then fixed in 4% paraformaldehyde in marine phosphate-buffered saline (PBS; 50 mM sodium phosphate buffer with 0.45 M NaCl; pH 7.4) overnight at 4°C. Animals were then rinsed four times for 30 min in marine PBS. Light organs were dissected and rinsed twice for 5 min in 1% Triton X-100 in marine PBS. The organs were then permeabilized for 2 days at 4°C in 1 ml of 1% Triton X-100 in marine PBS with mixing. They were then blocked overnight at 4°C in a solution of 1% Triton X-100, 1% goat serum, and 0.5% BSA in marine PBS. The organs were incubated with a 1:100 dilution of the antiactin polyclonal antibody (described above) in blocking solution for 2 weeks at 4°C. Samples were then rinsed four times for 1 h in 1% Triton X-100 in marine PBS and incubated overnight in blocking solution at 4°C. Rhodamine conjugated to goat anti-rabbit secondary antibody (Jackson Immunoresearch, West Grove, Pa.) was added at a 1:25 dilution to fresh blocking solution, and the samples were incubated in the dark overnight at 4°C. Samples were rinsed four times for 30 min in 1% Triton X-100 in marine PBS with two final rinses in marine PBS. Light organs were then mounted on glass slides in sterile 90% glycerol and viewed by confocal microscopy. As a control, for each time point cohorts of aposymbiotic and symbiotic samples were incubated as described above minus the primary antibody incubation step.

Determination of light organ mRNA levels. To characterize bacteria-induced changes in mRNA pools, we used both Northern blot analysis and real-time reverse transcriptase PCR (RT-PCR). For both methods, total RNA was extracted from light organs using TRIzol reagent (Gibco BRL, Rockville, Md.), and mRNA was then purified with an MPG mRNA purification kit (CPG, Lincoln Park, N.J.). Yield of RNA was spectrophotometrically determined, and both total RNA and mRNA were run on 2% agarose gels to assess the quality of the extraction and to serve as a loading control. Northern blotting was performed as previously described (37). For real-time RT-PCR, 50-μl RT reactions were done with avian myeloblastosis virus RT (Promega, Madison, Wis.), 300 ng of mRNA, and the reverse primer for actin. From the 50-μl RT reaction mixture, 1 μl was used per 10-μl PCR mixture. Three separate RNA purifications and RT reactions were conducted at each time point for both aposymbiotic and symbiotic light organs. A control without RT was included in each experiment to ensure that no genomic DNA was contaminating the sample. Real-time PCR was performed using an iCycler (Bio-Rad, Hercules, Calif.). Ten-microliter reaction mixtures contained a 0.2 μM concentration of primers and 3.0 mM $MgCl_2$ to amplify a 100-bp fragment. The product size and the amplification of a single product were confirmed by gel electrophoresis. SYBR Green, buffer, nucleotides, and *Taq* DNA polymerase were derived from the SYBR Green PCR core reagent kit (Perkin-Elmer Biosystems, Foster City, Calif.). PCR cycles were conducted as follows: 95°C for 10 min, followed by 40 cycles of 95°C for 15 s, 60°C for 10 s, and 72°C for 10 s. Standard curves were constructed using 10-fold dilutions of known starting amounts of the actin target. Actin primers used were as follows: forward, 5′-GAGCGTAAATACTCTGTC; reverse, 5′-AATGGATG GGCCGCACTCAT.

In situ hybridization. The sense and antisense riboprobes were made as previously described (21). Animals were anesthetized in 2% ethanol in seawater and fixed for 12 h in 4% paraformaldehyde in marine PBS at 4°C. Light organs were dissected from the mantle and rinsed three times for 10 min in 0.1% Tween 20–marine PBS (PTw). Specimens were refixed for 1 h at room temperature in 4% paraformaldehyde in PTw and then rinsed five times for 10 min in PTw. Samples were incubated for 10 min at room temperature in hybridization buffer (50% formamide, 100 μg of salmon sperm DNA/ml, 1% SDS, 0.1% Tween 20, 50 μg of heparin/ml, and 5× SSC [1× SSC is 0.15 M NaCl and 0.015 M sodium citrate; pH 7.4]). Each specimen was incubated overnight at 60°C in hybridization buffer. Digoxigenin-labeled probes (50 ng/μl of stock) were denatured at 90°C in hybridization buffer for 10 min. After denaturation, probes were added to fresh hybridization buffer at a concentration of 0.1 ng/μl. Samples were incubated overnight at 60°C, rinsed at 60°C for 20 min in 75% hybridization buffer–25% 2× SSC. They were then placed for 15 min in 50% hybridization buffer–50% 2× SSC, followed by 15 min in 25% hybridization buffer–75% 2× SSC, then 15 min in 100% 2× SSC, and finally twice for 30 min in 0.05× SSC. Samples were then rinsed at room temperature for 10 min in 75% 0.05× SSC–25% PTw, followed by 10 min in 50% 0.05× SSC–50% PTw, 10 min in 25% 0.05× SSC–25% PTw, and 10 min in 100% PTw. After rinsing, samples were blocked overnight at 4°C in marine PBS with 1% Triton X-100, 0.5% BSA, and 1% goat serum. Specimens were then incubated in alkaline phosphatase-conjugated sheep anti-digoxigenin Fab fragments (Boehringer-Mannheim, Indianapolis, Ind.) at a 1:500 dilution overnight at 4°C, washed three times for 10 min at room temperature in marine PBS with 0.2% Triton X-100 and 0.1% BSA, washed three times for 10 min in HNPP detection buffer (2-hydroxy-3-naphtoic acid-2′-phenylanilide phosphate [Roche Applied Sciences, Indianapolis, Ind.] in 100 mM Tris-HCl, 100 mM NaCl, 10 mM $MgCl_2$; pH 8), and then incubated for 2 h in HNPP-Fast Red TR substrate at room temperature according to the manufacturer's instructions. Samples were then rinsed four times for 10 min in marine PBS, mounted in 2% DABCO (1,4-diazabicyclo[2.2.2]octane) in 50% glycerol–marine PBS, and viewed by confocal microscopy.

Labeling with phalloidin. Animals were anesthetized in 2% ethanol and fixed in 4% formaldehyde in marine PBS for 1 h at room temperature. Light organs were dissected into fresh marine PBS, rinsed twice for 10 min in marine PBS, and then permeabilized in 1% Triton X-100 in marine PBS for 20 min. Permeabilized samples were stained overnight in 2 mg of rhodamine phalloidin/ml in 1% Triton X-100 in marine PBS, then rinsed three times for 10 min in marine PBS, and viewed by confocal microscopy.

Measurements of duct dimensions and determinations of duct epithelial cell number and shape. To stain duct cells in living animals, live specimens were placed for 30 min in a 5-ng/ml solution of acridine orange in seawater. Animals were then rinsed in seawater and anesthetized in 2% ethanol. The animals were ventrally dissected to reveal the light organ, and the circumference of the medial ducts was determined by confocal microscopy.

To investigate possible cellular mechanisms for change in duct dimensions, animal tissues of 48-h aposymbiotic and symbiotic animals were stained with rhodamine phalloidin (as described above) to study the number of cells lining the duct space and the shape of these cells.

RESULTS

Actin synthesis increased during the onset of the symbiosis. No reproducible differences in the steady-state profile of soluble proteins of 12-h aposymbiotic and symbiotic organs were detected in the present study (Fig. 2A), as previously shown (5). However, 2-D PAGE of ^{35}S-labeled proteins from 12-h light organs detected several newly synthesized proteins, some of which were different between aposymbiotic and symbiotic organs and some of which showed similar levels of synthesis (Fig. 2B). Strong labeling of two proteins at an M_r of ~42 and pI of ~5.1 to 5.2 suggested that they may be newly synthesized actin. Immunoblotting of the total soluble protein run in the

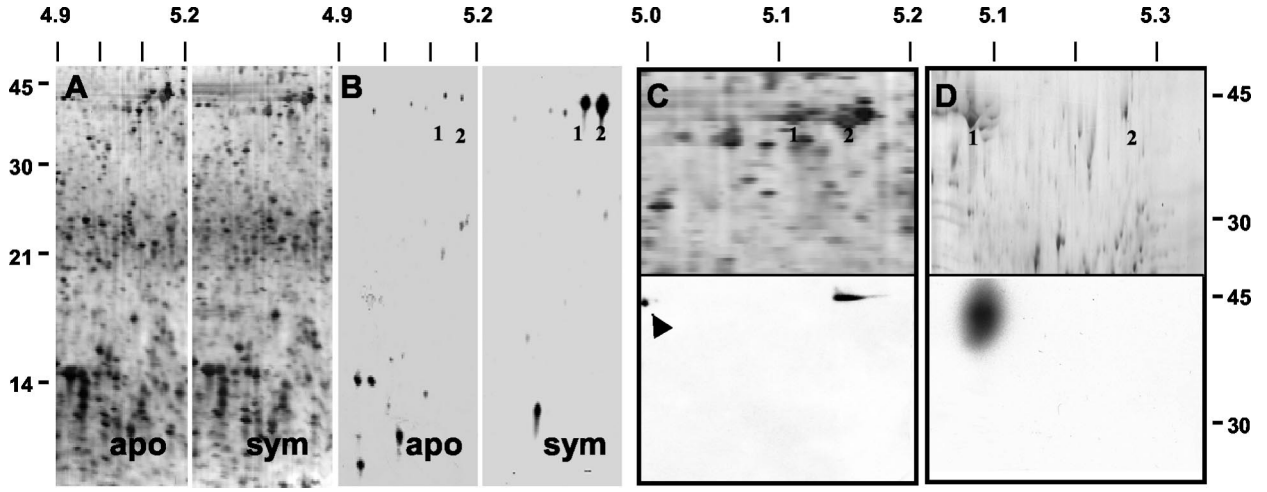

FIG. 2. Actin protein was more actively synthesized in 12-h symbiotic light organs. (A) Sectors of silver-stained, 2-D SDS-PAGE gels of soluble proteins (20 μg loaded on each gel) of 12-h aposymbiotic and symbiotic light organs. No reproducible differences in protein profiles could be detected by this method. (B) Autoradiograms of ^{35}S-labeled soluble proteins (20 μg loaded on each gel) of the light organs of aposymbiotic and symbiotic animals. Proteins at a pI and M_r consistent with actin (1, 2) were more actively synthesized in symbiotic animals. (C) Upper panel: sector of a silver-stained, 2-D SDS-PAGE gel of soluble proteins from the light organs of symbiotic animals resolved in the pI range from 4.0 to 7.0. Numbers (1, 2) correspond to those in panel B. Lower panel: immunoblot of the above 2-D gel using antiactin antibodies. Control actin (arrow) was loaded onto the second dimension as a control. (D) Upper panel: sector of a silver-stained, 2-D SDS-PAGE gel of soluble proteins from the light organs of symbiotic animals resolved in the pI range from 4.5 to 5.5. Numbers (1, 2) correspond to those in panel B. Lower panel: immunoblot of the above 2-D gel using antiactin antibodies. Antibody labeling demonstrated that the more acidic of the two proteins (1) at ~42 kDa was actin. Biotinylated standards were used to determine the M_r. Molecular mass markers for A and B and for C and D appear on the left and right, respectively. pI markers are along the top. apo = aposymbiotic; sym = symbiotic.

same pH range of these gels, i.e., pH 4 to 7, confirmed that one or both of these proteins were actin (Fig. 2C). Immunoblotting in which proteins were resolved across a narrower pH range (i.e., 4.5 to 5.5) indicated that only one of these two proteins was actin (Fig. 2D). At this resolution, the proteins ran at slightly different pIs.

Increases in actin abundance were localized to the apical surfaces of the duct epithelia. Immunocytochemistry was performed to determine where symbiont-induced changes in actin levels were occurring in the light organ. Although the antibody used in immunocytochemistry analyses recognized both muscle and cytoskeletal actin in the host light organ, differences in antibody cross-reactivity, as detected by fluorescence intensity, were not observed between aposymbiotic and symbiotic animals in the labeling of the muscles or other portions of the light organ (data not shown). However, significant differences were observed between aposymbiotic and symbiotic animals in actin levels in the epithelial cells lining the light organ ducts within 6 h of exposure of the symbiotic animals to *V. fischeri* (Fig. 3). The changes indicated an increase in actin in the microvillar surface and terminal web (Fig. 3A), the actin-rich region of the apical area of polarized epithelia. Beginning at the 6-h time point and continuing through 48 h, significant differences in immune cross-reactivity were detected in the duct between aposymbiotic and symbiotic animals (Fig. 3B). A significant increase in cross-reactivity was detected between 6- and 12-h symbiotic animals; thereafter, no significant differences were detected among the symbiotic animals at time points between 12 and 48 h. At 60 h, although the level of cross-reactivity for symbiotic ducts was on average slightly higher, it was not significantly different from that of aposymbiotic animals. No sig-

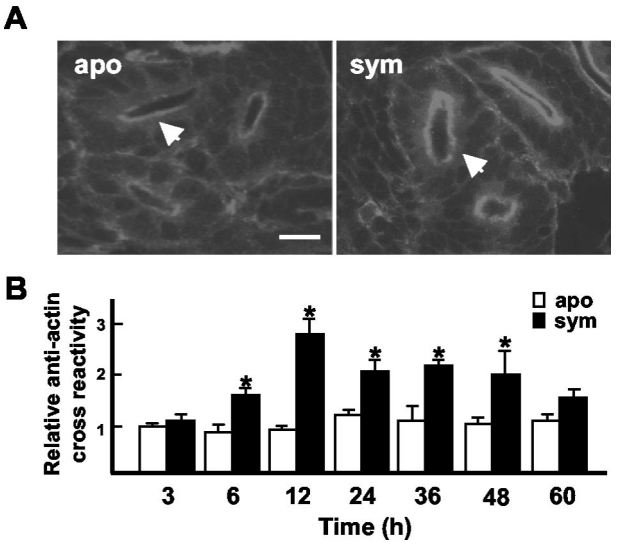

FIG. 3. The *V. fischeri*-induced changes in actin protein levels occurred in the duct epithelia. (A) Confocal micrographs of cross-sections of ducts of 12-h aposymbiotic and symbiotic light organs. Light organs were labeled with antiactin rhodamine-conjugated goat anti-rabbit antibody. The medial ducts (arrows) were used for fluorescence quantification. (B) Relative fluorescence of sites cross-reactive with antiactin antibodies in the medial ducts of aposymbiotic and symbiotic light organs over the first 60 h. For each condition, $n = 15$. Data are the mean ± the standard error of the mean. A * indicates a significant difference (analysis of variance followed by a Tukey's pairwise comparison; $P < 0.05$) between aposymbiotic and symbiotic samples. Bar, 25 μm. apo = aposymbiotic; sym = symbiotic.

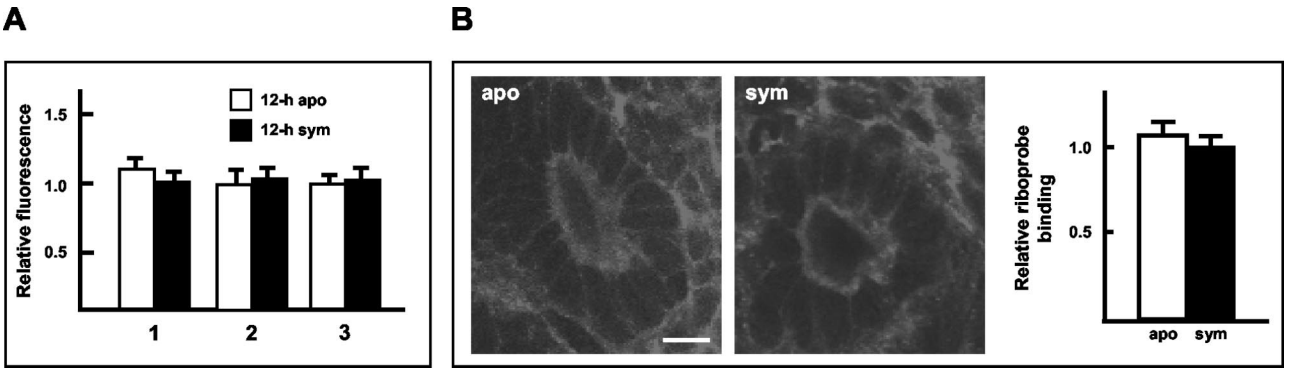

FIG. 4. mRNA abundance in the light organ of aposymbiotic and symbiotic light organs was not significantly different during the onset of the symbiosis. (A) Real time RT-PCR using actin-specific primers and mRNA from light organs of 12-h animals. Three independent mRNA pools (1 to 3) were extracted for each of the two conditions, and triplicate real-time RT-PCRs were conducted for each mRNA pool. For all PCR runs, standards run concurrently had a correlation coefficient of 1.0 ± 0.02 and a slope of -3.3 ± 0.2, indicating that the efficiency of the PCR was ~2, i.e., each PCR cycle yielded a twofold increase in product. No significant differences were detected between aposymbiotic and symbiotic mRNA within a given extraction trial (Student's t test; $P < 0.05$). (B) Confocal micrographs of localization of actin mRNA by in situ hybridization in 3-h light organs; similar results were obtained for samples at 6 and 12 h. The representative graph shows the relative fluorescence of hybridization to the actin antisense probes at 3 h. Data are the mean ± the standard error of the mean ($n = 6$). Bar, 15 μm. apo = aposymbiotic; sym = symbiotic.

nificant differences in actin cross-reactive sites were detected among the aposymbiotic cohorts. Incubation of animals in secondary antibody alone resulted in no detectable cross-reactivity above background.

Because the antiactin antibody recognizes both globular and filamentous actin, we used labeling with phalloidin, which recognizes only the latter, at the 48-h time point to determine whether the levels of filamentous actin changed during the onset of the symbiosis. This analysis provided evidence for a twofold increase in filamentous actin in symbiotic animals, suggesting that some of the change in actin protein was due to an increase in filamentous actin (Student's t test; $P < 0.05$; for an example of phalloidin staining patterns, see Fig. 7, below).

No changes in actin mRNA levels were detectable during the onset of the symbiosis. To determine whether symbiont-induced changes in actin were the result of changes at the level of transcription, we studied actin mRNA levels in whole light organs by real-time RT-PCR and Northern analysis and localized actin mRNA in light organs by in situ hybridization. No significant differences in actin mRNA levels were detected by real-time RT-PCR (Fig. 4A), Northern blot analyses (data not shown), or in situ hybridization in aposymbiotic and symbiotic light organs at 12 h (Fig. 4B). These data revealed that the significant changes in actin protein synthesis at 12 h in symbiotic animals were not coincident with detectable changes in message levels. Because symbiont-induced changes in mRNA levels may have occurred hours before changes in actin protein could be detected, we also performed in situ hybridization to localize actin mRNA in the light organs of 3- and 6-h aposymbiotic and symbiotic animals. No differences in actin mRNA could be detected in any part of the light organs, including the duct epithelia, at these time points (Fig. 4B). The sense probe controls did not bind to the tissues to produce fluorescence above background levels.

Persistent colonization with *V. fischeri* was required to maintain the changes in light organ actin. To determine whether *V. fischeri* delivers a signal that directs an irreversible change in the duct epithelia or produces a signal that must be constantly present to maintain the change, we performed experiments in which we cured the light organs after symbiont-induced changes had been induced (Fig. 5). CM was used to cure juveniles of their bacterial symbionts after 12 h of infection; the subsequent abundance of antiactin cross-reactivity in the duct epithelia at 48 h was not significantly different from those of the aposymbiotic juveniles at that time. CM treatment alone had no apparent pharmacological effect; the intensity of fluorescence due to cross-reactivity in hatchling squid infected with the CM-resistant strain of *V. fischeri* and subsequently treated

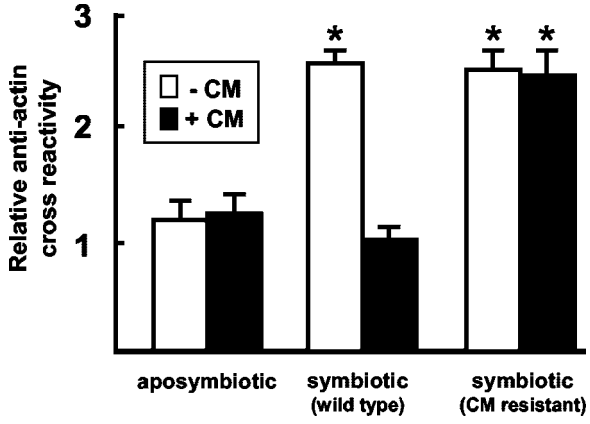

FIG. 5. Constant exposure to *V. fischeri* was required to maintain the symbiont-induced changes in actin. A representative experiment showing relative fluorescence of cross-reactive sites to antiactin in the medial ducts of 48-h juvenile light organs is shown. White bars indicate animals that had no exposure to CM. Solid bars indicate animals that were treated continuously with 20 μg of CM/ml in seawater starting at 12 h. Cohorts of animals that had been inoculated with a CM-resistant strain of *V. fischeri* [ES114(pVO8)] were used to control for effects of CM. For each condition, $n = 15$; data are the mean ± standard error of the mean. A * indicates a significant difference (analysis of variance followed by a Tukey's pairwise comparison; $P < 0.05$) between aposymbiotic animals (± CM) and symbiotic animals colonized by either wild type (± CM) or CM-resistant (± CM) strains of *V. fischeri*.

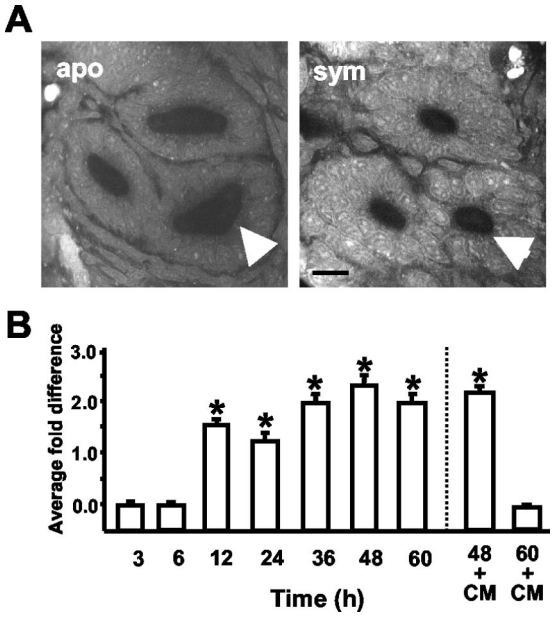

FIG. 6. Persistent colonization by *V. fischeri* induced changes in medial duct circumference. (A) Cross-sections through 48-h light organ ducts. The medial duct is indicated with an arrow. Bar, 20 μm. (B) Representative experiment showing the average fold differences, i.e., aposymbiotic dimensions divided by symbiotic dimensions, in the medial duct circumferences. In antibiotic curing experiments (right of the dashed line), cohorts of animals were treated continuously with 20 μg of CM/ml beginning at 12 h. For each condition, $n = 15$; data are the mean ± the standard error of the mean. A ∗ indicates a significant difference (Student's t test; $P < 0.05$) between aposymbiotic (apo) and symbiotic (sym) animals.

with CM was not significantly different from that of juveniles exposed to the wild-type strain. Taken together, these data demonstrated that constant exposure to *V. fischeri* is required to maintain the symbiont-induced changes in actin observed in the early hours of the symbiosis.

Increases in duct actin correlated with constriction of the ducts. We sought to determine whether a corresponding change in the architecture of the duct occurred with the observed increase in actin. Specifically, we asked whether duct circumference, epithelial cell number interfacing the duct space, and epithelial cell shape changed at various time points during the onset of the symbiosis. Commencing at 12 h, the average medial duct circumference of symbiotic animals was significantly smaller than that of aposymbiotic animals (Fig. 6). Antibiotic curing experiments revealed that this change in the ducts required persistent interaction with *V. fischeri*. However, the reversal of duct circumference to aposymbiotic levels after antibiotic treatment at 12 h was not apparent until 60 h, unlike the reversible changes in actin protein levels, which were apparent by 48 h (Fig. 6B).

The average number of cells lining the duct lumina of 48-h symbiotic animals was significantly lower than that of aposymbiotic animals (Fig. 7). Further, in aposymbiotic animals, the duct epithelia were a regular array of parallel columnar cells, whereas the shape of many of the duct cells in symbiotic animals was highly irregular, with narrow apical surfaces. These data suggested that the symbiont-induced decrease in duct circumference is a result of a reduction in the number of cells circumscribing the duct lumen and that reduction is due to displacement of cells away from the population comprising the duct epithelium.

DISCUSSION

The results of this study provide evidence that, similar to the action of some pathogenic microorganisms, a beneficial bacterial partner markedly influences the actin cytoskeleton of host cells. Beginning with the first exposure and continuing for the early days of the symbiosis, *V. fischeri* cells induced an increase in actin synthesis in the ducts, the passageway through which the symbionts enter during initial colonization and are expelled each day as part of the natural diel rhythm of the symbiosis. The increase in duct actin correlated with a decrease in the circumference of the duct. Thus, the symbionts enter the tissues and, by some unknown mechanism, narrow the entry way behind them.

Bacterial pathogens or symbionts usually affect the cytoskeletons of the cells with which they directly associate (8, 18). In contrast, the light organ ducts of *E. scolopes* are adjacent to, but not in direct contact with, the population of *V. fischeri* cells

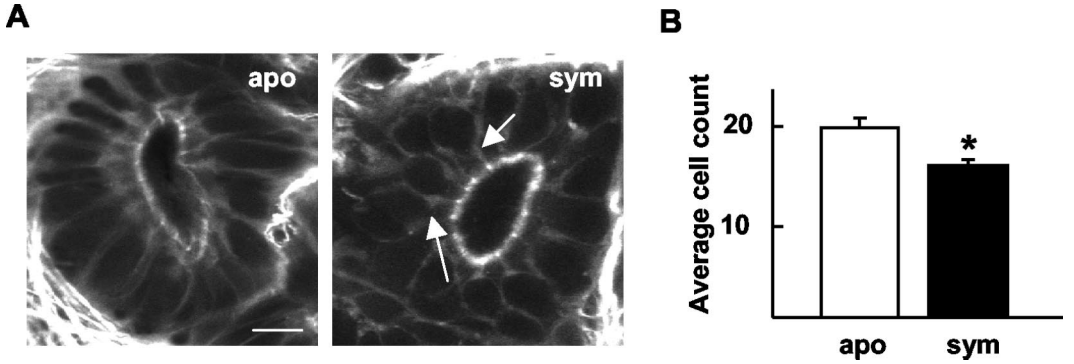

FIG. 7. Cells lining the medial ducts of 48-h symbiotic animals were fewer in number than in aposymbiotic animals. (A) Representative confocal micrograph showing a cross-section through a medial duct of a 48-h animal. Arrows indicate common cell shapes in the duct epithelia of symbiotic animals. Bar, 15 μm. (B) Cell counts through cross-sections of the medial ducts. Data are the mean ± the standard error of the mean ($n = 6$). A ∗ indicates a significant difference (Student's t test; $P < 0.05$). apo = aposymbiotic; sym = symbiotic.

in the crypts, except at the onset of the symbiosis and with venting each morning. Thus, either these brief, direct interactions are enough to cause the observed changes in the actin cytoskeleton or the products released from the symbiont population in the crypts are swept past the duct epithelial cells by the cilia lining the ducts. Alternatively, these cytoskeletal modifications in the duct cells could be signaled indirectly through the adjacent crypt epithelia, where the bacteria colonize. At present, it is not possible to identify experimentally which of these mechanisms is naturally occurring.

The changes observed in the duct appear to involve a complex array of factors, including an increase in actin synthesis and a reduction of duct circumference, accompanied by changes in duct cell shape and number. One interpretation of these data might be that the increase in actin protein in the apical surfaces of the ducts reflects a condensation or focusing of the preexisting actin pool. However, the evidence presented here supports an absolute change in actin synthesis. First, our 2-D gel data (Fig. 2) demonstrated such an increase, which was only detectable in the apical surfaces of the duct cells (Fig. 3). Second, significant increases in actin protein were first observed at 6 h, before a significant decrease in duct circumference was detectable (Fig. 3 and 6). And third, upon curing, the loss of actin cross-reactivity from the apical surfaces of the cells did not coincide in time with the reversal of duct dimension (Fig. 5 and 6).

We found that the increase in actin protein synthesis was not preceded by an increase in actin mRNA levels. Instead, our data suggest that the symbiont-induced changes are the consequence of posttranscriptional modifications. With rare exception (17), microbe-induced changes in actin gene transcription are unusual, as reported both in focused analyses of host cytoskeleton (for reviews, see references 1, 8, and 18) and in the more comprehensive microarray studies (16, 35, 38). However, it is possible in many such studies that small yet biologically significant changes have been disregarded because the actin gene is often used as a control gene, which may not always be a sound assumption (22).

Actin-mediated changes in tubule dimensions have been noted in the development of tissues of both invertebrates and vertebrates. For example, in the development of the tracheal system in *Drosophila melanogaster*, similar to the *E. scolopes* light organ ducts, the dimensions of the tracheal lumina change concomitantly with alterations in actin cytoskeleton in the apical surfaces of the tracheal epithelial cells (2). However, the mechanisms appear to differ. While the data suggest that changes in cell shape and a decrease in cell number are responsible for mediating the constriction of the light organ ducts, the developmental change in the tubules of the *Drosophila* tracheal system could be accounted for entirely by constriction in the apical cell surfaces of the tubule cells. Similarly, in a study of the development of salamander kidney tubules, a change in cell number also did not correlate with alterations in tubule size (6). The extent to which the symbiont-induced developmental program of the squid ducts is unusual, i.e., being mediated by a change in cell number, will require further comparative analyses.

These symbiont-induced developmental changes in the ducts add to the other known biomechanical and biochemical constraints, such as the activity of the cilia lining the duct (25) and the high concentration of toxic oxygen species (36; Davidson et al., Abstr. 101st Gen. Meet. Am. Soc. Microbiol., 2001), that the duct places on entry into host tissues. Further, this modification in the ducts is only one of a suite of effects that result from symbiont-directed shutdown of activities associated with the infection process. Once the symbiont has resided in the crypts for several hours, secretion of mucus from the superficial ciliated field ceases and, thus, further harvesting of potential symbiont cells no longer occurs (32). In addition, the symbionts induce the complete regression of the superficial ciliated field over 4 to 5 days (27). Together, the cessation of harvesting, loss of the superficial field, and constriction of the duct appear to act in concert to render the organ less susceptible to subsequent colonization.

The results of this study present two principal questions: (i) what is the bacterial signal that induces changes in the duct cells, and (ii) by what mechanisms do bacteria change the host cytoskeleton? The bacterial effectors known to induce changes in the cytoskeleton of animal hosts are most often specific toxins (1). The genome sequence of *V. fischeri* has revealed the presence of a gene encoding an ortholog of RTX, an actin cross-linking toxin in *Vibrio cholerae* (7), and may reveal orthologs of other toxins known to influence the actin cytoskeleton. Characterizations of the duct cell responses will provide an interesting comparison of the ways in which host cells respond to pathogens and beneficial symbionts. Most often, bacteria are reported to alter preexisting actin protein by directly or indirectly, covalently or noncovalently, modifying the actin cytoskeleton (1, 3, 18). Among other effects, pathogens are known to ADP-ribosylate actin in a covalent modification of the molecule, affect actin nucleation through the ARP 2/3 complex, or modulate actin cytoskeleton through modifying Rho GTPases (1). It is possible that similar molecular responses will be involved in the squid-vibrio system, but because outcomes of pathogenic and beneficial interactions are diametrically opposed, additional or different mechanisms may be operating. The ongoing production of expressed sequence tag libraries from the host light organs, characteristic of different times in the developmental program and of development under symbiotic and aposymbiotic conditions, should be immensely helpful in our quest to understand such complex interactions. With these molecular tools, we should be able to identify candidate genes and characterize their role in the dynamics of the symbiosis between the host squid and its beneficial bacterial partner.

ACKNOWLEDGMENTS

We thank W. Crookes, M. Goodson, B. Janssens, T. Koropatnick, E. G. Ruby, J. Stewart, and J. Troll for helpful discussions and comments on the manuscript. Histological and electron micrographs used in this orientation figure were donated by J. Foster.

This research was funded by NSF IBN 0211673 (to M.M.-N. and E. G. Ruby), NIH AI 50611 (to M.M.-N.), and NIH RR12294 (E. G. Ruby with M.M.-N.) and by a grant from the W. M. Keck Foundation (to E. P. Greenberg, with M.M.-N., E. G. Ruby, M. Apicella, and M. Welsh).

REFERENCES

1. **Barbieri, J. T., M. J. Riese, and K. Aktories.** 2002. Bacterial toxins that modify the actin cytoskeleton. Annu. Rev. Cell Dev. Biol. **18:**315–344.
2. **Beitel, G. J., and M. A. Krasnow.** 2000. Genetic control of epithelial tube size in the Drosophila tracheal system. Development **127:**3271–3282.

3. **Dantan-Gonzalez, E., Y. Rosenstein, C. Quinto, and F. Sanchez.** 2001. Actin monoubiquitylation is induced in plants in response to pathogens and symbionts. Mol. Plant-Microbe Interact. **14:**1267–1273.
4. **Doino, J. A., and M. J. McFall-Ngai.** 1995. A transient exposure to symbiosis-competent bacteria induces light organ morphogenesis in the host squid. Biol. Bull. **189:**347–355.
5. **Doino Lemus, J. A., and M. J. McFall-Ngai.** 2000. Alterations in the proteome of the *Euprymna scolopes* light organ in response to symbiotic *Vibrio fischeri.* Appl. Environ. Microbiol. **3:**603–607.
6. **Fankhauser, G.** 1945. Maintenance of normal structure in heteroploid salamander larvae, through compensation of changes in cell size by adjustment of cell number and cell shape. J. Exp. Zool. **93:**913–915.
7. **Fullner, K. J., W. I. Lencer, and J. J. Mekalanos.** 2001. *Vibrio cholerae*-induced cellular responses of polarized T84 intestinal epithelial cells are dependent on production of cholera toxin and the RTX toxin. Infect. Immun. **69:**6310–6317.
8. **Goldberg, M. B.** 2001. Actin-based motility of intracellular microbial pathogens. Microbiol. Mol. Biol. Rev. **65:**595–626.
9. **Goosney, D. L., M. de Grado, and B. B. Finlay.** 1999. Putting *E. coli* on a pedestal: a unique system to study signal transduction and the actin cytoskeleton. Trends Cell Biol. **9:**11–14.
10. **Graf, J.** 2000. Symbiosis of *Aeromonas* and *Hirudo medicinalis*, the medicinal leech. ASM News **66:**147–153.
11. **Graf, J., P. V. Dunlap, and E. G. Ruby.** 1994. Effect of transposon-induced motility mutations on colonization of the host light organ by *Vibrio fischeri.* J. Bacteriol. **176:**6986–6991.
12. **Graf, J., and E. G. Ruby.** 1998. Characterization of the nutritional environment of a symbiotic light organ using bacterial mutants and chemical analyses. Proc. Natl. Acad. Sci. USA **95:**1818–1822.
13. **Henderson, B., M. Wilson, R. McNab, and J. L. Alistar.** 1999. Cellular microbiology: bacteria-host interactions in health and disease. John Wiley and Sons, Chicester, England.
14. **Hooper, L. V., L. Bry, P. G. Falk, and J. I. Gordon.** 1998. Host-microbial symbiosis in the mammalian intestine: exploring an internal ecosystem. Bioessays **20:**336–343.
15. **Hooper, L., and J. I. Gordon.** 2001. Commensal host-bacterial relationships in the gut. Science **292:**1115–1118.
16. **Hooper, L., M. Wong, A. Thelin, L. Hansson, P. Falk, and J. I. Gordon.** 2001. Molecular analysis of commensal host-microbial relationships in the intestine. Science **291:**881–884.
17. **Jin, S., R. Xu, Y. Wei, and P. H. Goodwin.** 1999. Increased expression of a plant actin gene during a biotrophic interaction between round-leaved mallow, *Malva pusilla*, and *Colletotrichum gloeosporioides* f. sp. *malvae.* Planta **209:**487–494.
18. **Kazmierczak, B. I., K. Mostov, and J. N. Engel.** 2001. Interaction of bacterial pathogens with polarized epithelium. Annu. Rev. Microbiol. **55:**407–435.
19. **Kimbell, J. R., M. J. McFall-Ngai, and G. Roderick.** 2002. Two genetically distinct populations of bobtail squid, exist on the island of Oahu. Pac. Sci. **56:**347–355.
20. **Kimbell, J. R., and M. J. McFall-Ngai.** 2003. The squid-vibrio symbioses: from demes to genes. Integr. Comp. Biol. **4:**254–260.
21. **Lamarcq, L., and M. J. McFall-Ngai.** 1998. Induction of a gradual, reversible morphogenesis of its host's epithelial brush border by *Vibrio fischeri.* Infect. Immun. **66:**777–785.
22. **Lupberger, J., K. A. Kreuzer, G. Baskaynak, U. R. Peters, P. le Coutre, and C. A. Schmidt.** 2002. Quantitative analysis of beta-actin, beta-2-microglobulin, and porphobilinogen deaminase mRNA and their comparison as control transcripts for RT-PCR. Mol. Cell. Probes **16:**25–30.
23. **McFall-Ngai, M. J.** 1999. Consequences of evolving with bacterial symbionts: insights from the squid-vibrio associations. Annu. Rev. Ecol. Syst. **301:**235–256.
24. **McFall-Ngai, M. J., and E. G. Ruby.** 1991. Symbiont recognition and subsequent morphogenesis as early events in an animal-bacterial mutualism. Science **254:**1491–1494.
25. **McFall-Ngai, M. J., and E. G. Ruby.** 1998. Squids and vibrios: when first they meet. BioScience **48:**257–265.
26. **Montgomery, M. K., and M. J. McFall-Ngai.** 1993. Embryonic development of the light organ of the sepiolid squid *Euprymna scolopes* Berry. Biol. Bull. **184:**296–308.
27. **Montgomery, M. K., and M. J. McFall-Ngai.** 1994. Bacterial symbionts induce host organ morphogenesis during early postembryonic development of the squid *Euprymna scolopes.* Development **120:**1719–1729.
28. **Nishiguchi, M. K., E. G. Ruby, and M. J. McFall-Ngai.** 1998. Competitive dominance among strains of luminous bacteria provides an unusual form of evidence for parallel evolution in the sepiolid squid-vibrio symbioses. Appl. Environ. Microbiol. **64:**3209–3213.
29. **Nyholm, S. V., and M. J. McFall-Ngai.** 1998. Sampling the microenvironment of the *Euprymna scolopes* light organ: description of a population of host cells with the bacterial symbiont *Vibrio fischeri.* Biol. Bull. **195:**89–97.
30. **Nyholm, S. V., and M. J. McFall-Ngai.** 2003. Dominance of *Vibrio fischeri* in secreted mucus outside the light organ of *Euprymna scolopes*: the first site of symbiont specificity. Appl. Environ. Microbiol. **69:**3932–3937.
31. **Nyholm, S. V., E. V. Stabb, E. G. Ruby, and M. J. McFall-Ngai.** 2000. Harvesting symbiotic vibrios: imposing a magnet on the environmental haystack. Proc. Natl. Acad. Sci. USA **97:**10231–10294.
32. **Nyholm, S. V., B. Deplancke, H. R. Gaskins, M. A. Apicella, and M. J. McFall-Ngai.** 2002. Roles of *Vibrio fischeri* and nonsymbiotic bacteria in the dynamics of mucus secretion during symbiont colonization of the *Euprymna scolopes* light organ. Appl. Environ. Microbiol. **68:**5113–5122.
33. **Roberts, F. A., and R. P. Darveau.** 2000. Beneficial bacteria of the periodontium. Periodontology **30:**40–50.
34. **Rook, G. A., and J. L. Stanford.** 1998. Give us this day our daily germs. Immunol. Today **19:**113–116.
35. **Rosenberger, C. M., M. G. Scott, M. R. Gold, R. F. Hancock, and B. B. Finlay.** 2000. *Salmonella typhimurium* infection and lipopolysaccharide stimulation induce similar changes in macrophage gene expression. J. Immunol. **164:**5894–5904.
36. **Ruby, E. G., and M. J. McFall-Ngai.** 1999. The many roles of oxygen in the symbiotic bacterial colonization of an animal epithelium. Trends Microbiol. **7:**414–419.
37. **Tomarev, S. I., R. D. Zinovieva, V. M. Weis, A. B. Chepelinsky, J. Piatigorsky, and M. J. McFall-Ngai.** 1993. Abundant mRNAs in the squid light organ encode proteins with high similarity to mammalian peroxidases. Gene **132:** 219–226.
38. **Vaena de Avalos, S., I. J. Blader, M. Fisher, J. C. Boothroyd, and B. Burleigh.** 2001. Immediate/early response to *Trypanosoma cruzi* infection involves minimal modulation of host cell transcription. J. Biol. Chem. **277:**630–644.
39. **Visick, K. L. and E. G. Ruby.** 1997. New genetic tools for use in the marine bioluminescent bacterium *Vibrio fischeri*, p. 119–122. *In* J. W. Hastings, L. J. Kricka, and P. E. Stanley (ed.), Bioluminescence and chemiluminescence. Wiley and Sons, New York, N.Y.
40. **Visick, K. L., and M. J. McFall-Ngai.** 2000. An exclusive contract: specificity in the *Vibrio fischeri-Euprymna scolopes* partnership. J. Bacteriol. **182:**1779–1787.
41. **Visick, K. L., J. S. Foster, J. Doino Lemus, M. J. McFall-Ngai, and E. G. Ruby.** 2000. *Vibrio fischeri lux* genes play an important role in colonization and development of the host light organ. J. Bacteriol. **182:**4578–4586.